
Bi-directional Weakly Supervised Knowledge Distillation for Whole Slide Image Classification

Linhao Qu*

Digital Medical Research Center,
School of Basic Medical Science,
Fudan University
lhqu20@fudan.edu.cn

Xiaoyuan Luo*

Digital Medical Research Center,
School of Basic Medical Science,
Fudan University
19111010030@fudan.edu.cn

Manning Wang†

Digital Medical Research Center,
School of Basic Medical Science,
Fudan University
mnwang@fudan.edu.cn

Zhijian Song†

Digital Medical Research Center,
School of Basic Medical Science,
Fudan University
zjsong@fudan.edu.cn

Abstract

Computer-aided pathology diagnosis based on the classification of Whole Slide Image (WSI) plays an important role in clinical practice, and it is often formulated as a weakly-supervised Multiple Instance Learning (MIL) problem. Existing methods solve this problem from either a bag classification or an instance classification perspective. In this paper, we propose an end-to-end weakly supervised knowledge distillation framework (WENO) for WSI classification, which integrates a bag classifier and an instance classifier in a knowledge distillation framework to mutually improve the performance of both classifiers. Specifically, an attention-based bag classifier is used as the teacher network, which is trained with weak bag labels, and an instance classifier is used as the student network, which is trained using the normalized attention scores obtained from the teacher network as soft pseudo labels for the instances in positive bags. An instance feature extractor is shared between the teacher and the student to further enhance the knowledge exchange between them. In addition, we propose a hard positive instance mining strategy based on the output of the student network to force the teacher network to keep mining hard positive instances. WENO is a plug-and-play framework that can be easily applied to any existing attention-based bag classification methods. Extensive experiments on five datasets demonstrate the efficiency of WENO. Code is available at <https://github.com/miccaiif/WENO>.

1 Introduction

Histopathological images play an important role in cancer diagnosis and prognosis prediction [23, 31, 30, 20], and they can be scanned by digital slide scanners into Whole Slide Images (WSIs), which facilitates the development of deep learning-based automatic analysis techniques. However, there are two challenges in deep learning-based WSI analysis. First, WSIs have huge resolutions, typically reaching $100,000 \times 100,000$ pixels, and thus cannot be directly input into deep models. For this reason, WSIs are usually tiled into many small patches for processing. Second, fine-grained

*Equal Contribution.

†Corresponding Authors. All authors are also from Shanghai Key Lab of Medical Image Computing and Computer Assisted Intervention.

(patch-level) annotation is very time-consuming and labor-intensive, and usually pathologists can only provide slide-level labels, so traditional supervised learning methods cannot be directly used. Therefore, WSI classification is often formulated as a deep multiple instance learning (MIL) problem, which is a weakly supervised learning paradigm [30, 26, 4, 35].

In the MIL paradigm, each WSI is considered as a bag, and the patches cut out of it are considered as its instances. If a bag is negative, all the instances in it are negative, while if a bag is positive, at least one positive instance exists in it. Typically, deep MIL-based WSI classification performs two main tasks: bag classification and instance classification, which are used for automatic clinical diagnosis and positive region localization, respectively.

Currently, deep MIL-based WSI classification methods can be mainly classified into instance-based approach and bag-based approach. The instance-based approach [2, 5] first trains an instance classifier and then aggregates the predictions of each instance in a bag to obtain the bag prediction [7, 32, 33]. Because of the lack of patch-level labels, it is not known which patches are truly positive, so instance-based approach needs to select some patches from positive slides and assign them pseudo positive labels for training an instance classifier. The main problem of this approach is that the **pseudo instance labels contain a lot of noise**, which limits the performance of the trained instance classifier, and thus leads to inaccurate instance and bag classification.

The more common bag-based approach [13, 9, 38, 36, 29, 18, 27, 19, 28, 22] first extracts the features of each instance in a bag and aggregates the instance features to obtain the bag feature using a trainable attention mechanism. Then, a bag classifier is trained in a supervised manner. During inference, the bag classifier is used to perform bag classification and the attention scores can be utilized to measure the contribution of each instance to bag classification so as to perform the instance classification. However, this bag-based approach suffers from two serious problems: **1) Poor performance of instance classification.** Different positive instances have different levels of difficulty of being recognized. The classifier is trained on bag-level loss, so it can correctly recognize a positive bag by giving high attention weights to only a few easily recognized positive instances, while the harder ones are ignored. This makes the network tend to accurately classify only a few easy positive instances in the positive bags and lack the motivation to accurately classify the hard instances [29]. **2) Bias of the bag classifier.** For the same reason, the trained bag-classifier will have difficulty to generalize on bags that contain only hard positive instances.

To address the above issues, we propose an end-to-end **weakly supervised knowledge distillation framework (WENO)** for whole slide image classification. WENO integrates a bag classifier and an instance classifier in a knowledge distillation framework to mutually improve the performance of both classifiers by effective knowledge transfer between them. To the best of our knowledge, the concept of weakly supervised knowledge distillation is proposed for the first time. Figure 1 concisely illustrates the existing knowledge distillation paradigms and the principle of WENO proposed in this paper. Specifically, WENO contains a bag classifier based on the attention mechanism as the teacher branch and an instance classifier as the student branch. **To address the problem of poor instance classification performance**, we use the normalized attention scores of the teacher network as the soft pseudo labels of the instances in the positive bags to train the student branch through knowledge distillation, which alleviates the noisy pseudo label problem in previous instance-based methods. At the same time, since all the instances in negative bags are negative, they are also used in training the student branch to further improve its instance classification performance. Notably, different from common knowledge distillation methods in Figure 1 (a) and (b), we not only train the student branch but also train the teacher branch using the bag labels of WSIs. Moreover, we share the instance feature extractor of the student and the teacher to further enhance the knowledge transfer between the two branches. **To further address the problem of bias in the bag classifier**, we propose a hard positive instance mining (HPM) strategy. In particular, we use the knowledge learned by the student instance classifier to construct bags with less easy instances, forcing the teacher network to keep mining hard positive instances in positive bags.

The advantages of our method are:

- We propose a weakly supervised knowledge distillation framework, WENO, for WSI classification. WENO integrates a bag classifier and an instance classifier in a knowledge distillation framework to mutually improve the performance of both classifiers by two-way knowledge transfer between them.

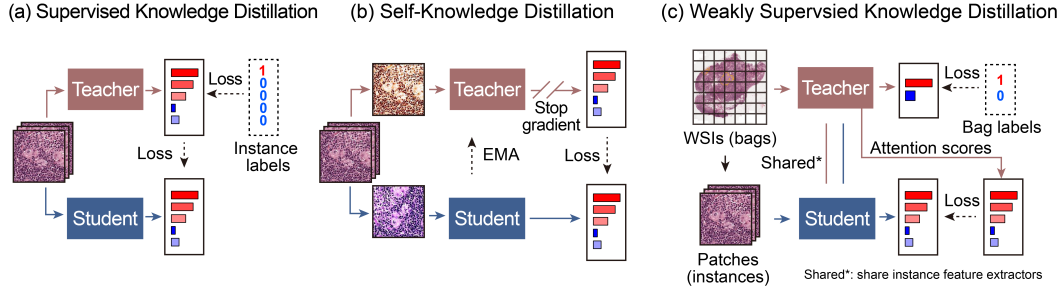


Figure 1: Architecture of common existing knowledge distillation frameworks and the proposed weakly supervised knowledge distillation framework. In traditional supervised knowledge distillation (a), the teacher network is trained in advance and it keeps unchanged during training the student. Knowledge is distilled from the teacher to the student. In recent self-knowledge distillation (b), such as DINO [3], the teacher has the same architecture with the student and it is not trainable but updated from the student. Two-way knowledge transfer exists between the teacher and the student. In comparison, in our proposed framework (c), the teacher is a bag-classifier and it is also trained with weak slide-level labels. Knowledge is distilled from teacher to student by providing pseudo instance labels using attention scores of the teacher and knowledge transfer from the student to the teacher is achieved by sharing instance feature extractors between them.

- We further propose a hard positive instance mining (HPM) strategy to force the teacher network to continuously learn and mine hard positive instances in positive bags, thus alleviating the problem of focusing on easy positive instances in bag-based methods.
- WENO is a plug-and-play framework that can be conveniently applied to any existing bag-based methods using attention mechanism to improve their performance of both instance and bag classification. Extensive experiments on five datasets show that the current SOTA methods ABMIL [13] and DSMIL [18] achieve significant improvements in both instance and bag classification performance when they are combined with WENO. Code will be publicly available.

2 Related Work

2.1 Deep Multiple Instance Learning

Instance-based methods Instance-based methods focus on training an instance classifier and then aggregating the instance predictions in a bag to make the bag prediction. For example, Campanella et al. [2] and Chikontwe et al. [5] iteratively trained the instance classifier by selecting key instances based on the predicted probability of the instance classifier in each iteration and assigning them pseudo labels of the corresponding bags. After that, the former used Recurrent Neural Network (RNN) to aggregate instance predictions to perform bag classification, and the latter proposed a soft-assignment strategy for bag inference.

Bag-based methods Bag-based methods focus on aggregating instance features in a bag into a bag feature, and then training a bag classifier with bag labels. Most of them utilize attention mechanism to aggregate instance features, in which Ilse et al. [13] is the first work of this kind. Later, Hashimoto et al. [9] used the attention mechanism to aggregate instance features at different resolutions. Yao, Zhu et al. [38, 36] proposed to first cluster the instances in each bag and then use the attention mechanism to aggregate the features of different clusters. Shi et al. [29] added the instance-level loss to the bag-level loss of [13], but the pseudo labels of each instance still came from its corresponding bag label. Recently, Li et al. [18] proposed to use non-local attention to aggregate instance features. Shao et al. [27], Li et al. [19] proposed to use Transformer to aggregate instance features.

Different from previous MIL methods, we construct a weakly supervised knowledge distillation framework to combine the training of a bag classifier and an instance classifier and utilize the knowledge transfer between the two branches of the distillation framework to mutually enhance both classifiers.

2.2 Knowledge Distillation

Knowledge distillation is originally a method to transfer knowledge from a pre-trained complex teacher network to a simpler student network. In the deployment phase, the student network can replace the teacher network to achieve model compression [25, 24, 21, 6, 11]. A common method of distilling knowledge from the teacher network to the student network is to use the output logits of the teacher network as the soft labels for training the student network [12].

Recently, self-distillation techniques are developed to train a student network without a pre-trained teacher network [17, 34, 37, 3]. Instead, the teacher usually has the same structure as the student and is updated by momentum-based moving average of the student network [3]. Figure 1 (a) and (b) concisely illustrates the two main existing knowledge distillation paradigms.

Knowledge distillation is a fast-developing area and we refer to [8] for a comprehensive survey. In this paper, we propose the concept of weakly supervised knowledge distillation for the first time.

3 Method

3.1 Problem Formulation

3.1.1 Multiple Instance Learning (MIL)

Given a dataset $W = \{W_1, W_2, \dots, W_N\}$ consisting of N WSIs, each WSI W_i is tiled into non-overlapping small patches $\{p_{i,j}, j = 1, 2, \dots, n_i\}$, where n_i is the number of patches cut out of W_i . All patches $p_{i,j}$ in W_i form a bag, where each patch is an instance. The bag label $Y_i \in \{0, 1\}$, $i = \{1, 2, \dots, N\}$ and the instance labels $\{y_{i,j}, j = 1, 2, \dots, n_i\}$ have the following relationship:

$$Y_i = \begin{cases} 0, & \text{if } \sum_j y_{i,j} = 0 \\ 1, & \text{else} \end{cases} \quad (1)$$

That is, all instances in negative bags are negative, while at least one positive instance exists in a positive bag. In MIL, only the labels of the training bags are available, while the labels of the instances in each positive bag are unknown. Our objective is to accurately predict both the labels of each bag in the test set (bag classification) and the labels of each instance in them (instance classification).

3.1.2 Bag-based MIL Methods

We first briefly review bag-based methods for easier understanding of our proposed framework. These methods first use an encoder f to extract features $z_{i,j}$ for all instances $\{p_{i,j}, j = 1, 2, \dots, n_i\}$ in bag W_i , and then aggregate these instance features using a permutation invariant function g to obtain the bag feature Z_i :

$$Z_i = g(f(p_{i,1}), f(p_{i,2}) \dots) \quad (2)$$

Finally, a bag classifier φ is utilized to predict the class of the bag.

$$\hat{Y}_i = \varphi(Z_i) \quad (3)$$

Traditional aggregation functions g include max-pooling and mean-pooling, while ABMIL [13] presents an attention-based trainable aggregation function:

$$Z_i = \sum_{j=1}^{n_i} a_{i,j} f(p_{i,j}) \quad (4)$$

$$a_{i,j} = \frac{\exp\{w^\top \tanh(Vh_{i,j}^\top)\}}{\sum_{j=1}^{n_i} \exp\{w^\top \tanh(Vh_{i,j}^\top)\}} \quad (5)$$

where $a_{i,j}$ is the attention score predicted by the self-attention network which is parameterized by w and V . The subsequent bag-based methods almost all adopt the attention-based aggregation methods, and the difference lies in how to construct the attention weight $a_{i,j}$. The weights $a_{i,j}$ reflect the

contribution of each instance in making the bag prediction, and they can be normalized as the instance prediction for positive bags.

$$\hat{y}_{i,j} = \text{norm}(a_{i,j}) \quad (6)$$

The normalization function can be formulated as follows:

$$X_{\text{norm}} = \frac{X - X_{\min}}{X_{\max} - X_{\min}} \quad (7)$$

where X_{norm} is the normalized data, X is the original data, and X_{\max} and X_{\min} are the maximum and minimum values of the original data, respectively.

3.2 Weakly Supervised Knowledge Distillation Framework

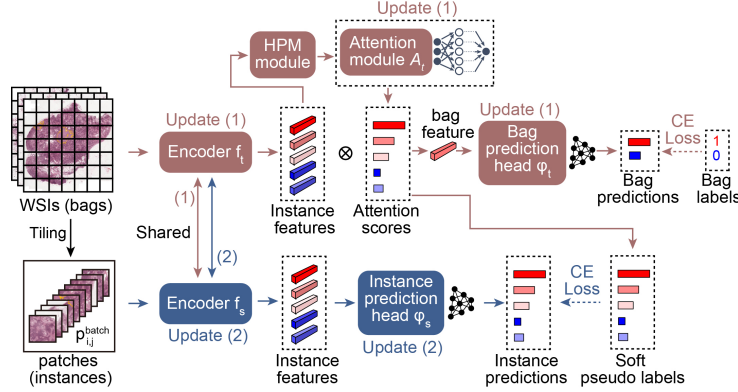


Figure 2: Architecture of the proposed **weakly supervised knowledge distillation (WENO)** framework. WENO contains a teacher branch (the red branch) and a student branch (the blue branch). The teacher branch is essentially a bag-level classifier, which consists of an instance encoder, a hard positive instance mining (HPM) module, an attention module and a bag prediction head. The student branch is essentially an instance-level classifier, which consists of an instance encoder and an instance prediction head. The two branches share the same instance encoder. The teacher branch is trained with bag labels, while the student branch is trained with the attention scores of the teacher branch as soft pseudo labels for the instances in positive bags. Furthermore, we propose a hard positive instance mining strategy (the HPM Module) to leverage the knowledge learned by the student to help the teacher learn hard positive instances. Note that the teacher branch and the student branch are optimized alternately, where the optimization of the teacher branch is represented by update (1) in the figure and the optimization of the student branch is represented by update (2) in the figure.

3.2.1 Framework Overview

Figure 2 illustrates the overall framework of our proposed WENO, which contains a teacher branch (the red branch) and a student branch (the blue branch). The whole teacher branch is a bag classifier, which consists of an instance encoder, a hard positive instance mining (HPM) module, an attention module and a bag prediction head. The whole student branch is an instance classifier, which consists of an instance encoder and an instance prediction head. The encoders in the two branches share the same parameters. We directly train the bag classifier in the teacher branch with bag labels. The instance classifier in the student branch is trained with two sets of instances, in which the first set is negative instances from negative bags and the second set is the instances from positive bags with pseudo labels generated according to the normalized attention scores output by the bag classifier in the teacher branch.

Different from the traditional distillation methods in which the teacher is pre-trained or updated by momentum updates from the student, our teacher and student models are trained alternately, so that not only the teacher can transfer the knowledge learned from the bag labels to the student, but also the knowledge learned by the student can be transferred to the teacher through the shared encoder. Furthermore, we propose the hard positive instance mining strategy (the HPM Module) to help the teacher better explore hard positive instances using the knowledge learned by the student, and further improve the network’s generalization ability for bag classification.

3.2.2 Teacher Network

The teacher branch is a typical bag classifier and one bag is input to it at a time. The instance features $z_{i,j}$ are first extracted using the encoder f_t for all instances $\{p_{i,j}, j = 1, 2, \dots, n_i\}$ within the bag W_i , and then filtered by the hard positive instance mining (HPM) module (See Section 3.3 for details), and then the attention score $a_{i,j}$ for each instance $z_{i,j}$ is obtained by the attention module A_t . Finally, the bag feature Z_i is obtained by aggregating the instance features within the bag using attention scores, and input to the bag prediction head φ_t to obtain the bag-level prediction \hat{Y}_i . Since the bag label Y_i is available, the teacher branch can be trained in an end-to-end manner.

$$z_{i,j} = f_t(p_{i,j}) \quad (8)$$

$$a_{i,j} = A_t(z_{i,j} \mid z_{i,1}, z_{i,2}, \dots, z_{i,n_i}) \quad (9)$$

$$Z_i = \sum_{j=1}^{n_i} a_{i,j} z_{i,j} \quad (10)$$

$$\hat{Y}_i = \varphi_t(Z_i) \quad (11)$$

$$\text{Loss}_{\text{teacher}} = CE(Y_i, \hat{Y}_i) \quad (12)$$

The purpose of training the bag-level classifier in the teacher branch is to obtain the attention scores of each instance and use them as soft pseudo labels to train the instance-level classifier in the student branch. Note that the teacher branch can be implemented with any existing bag-based MIL methods using attention mechanism, such as ABMIL [13], DSMIL [18], and TransMIL [27], etc., and we compare the performance of using ABMIL and DSMIL as the teachers in experiments (Section 4.5 and 4.6).

3.2.3 Student Network

The student branch is an instance-level classifier which consists of an encoder f_s shared with the teacher branch and an instance prediction head φ_s . We train the student branch using both the instances in positive bags with the normalized attention scores of the teacher classifier as soft pseudo labels and the instances in negative bags with true negative labels. Different from the teacher branch, the inputs to the student branch are randomly selected instances, which may come from the same bags or different bags.

The loss function of the student branch is the cross-entropy between the network prediction $\hat{y}_{i,j}$ and the label $y_{i,j}$:

$$y_{i,j} = \begin{cases} \text{norm}(a_{i,j}), & \text{if } Y_i = 1 \\ 0, & \text{else} \end{cases} \quad (13)$$

$$\hat{y}_{i,j} = \varphi_s(z_{i,j}) \quad (14)$$

$$\text{Loss}_{\text{student}} = CE(y_{i,j}, \hat{y}_{i,j}) \quad (15)$$

Since the student not only learns from the teacher’s attention scores, but also learns from the true negative instances directly, the instance classification ability of the student can surpass the attention scores of the teacher, which is supported by our experimental results (Section 4.5, 4.6 and 5). Moreover, since the student and the teacher share the parameters of the instance encoders, the knowledge learned by the student can also improve the instance-level classification ability of the teacher, which is also validated in the ablation study (Section 5).

In inference, we use the instance classifier in the student branch to make predictions for all instances in a bag, and then use a simple max-pooling to aggregate the predictions of instances to accomplish bag prediction.

3.3 Hard Positive Instance Mining Strategy (HPM)

Positive bags contain multiple positive instances, but they differ significantly in the difficulty of identification (e.g., in cancer detection, some patches contain a large number of cancer cells, while some other patches contain a small number of cancer cells). The loss of the bag-based methods is defined at the bag-level, so it only needs to identify at least one positive instance to classify the positive bag correctly. This makes bag-level classifiers tend to learn only easy positive instances but ignore the hard ones during training, which limits both the bag and the instance classification performance. To address this problem, we propose the hard positive instance mining strategy to force the teacher network to continuously learn and mine hard positive instances in the positive bags.

Specifically, we first train the teacher and the student models for a certain number of epochs, after which the student network has a certain instance classification capability. Then, before continuing to train the teacher, we use the student classifier to predict all the instances in the input positive bags, and drop some instances for which the student outputs high positive prediction probability to construct hard pseudo bags. In this way, we can force the bag classifier to keep mining hard positive instances in positive bags to achieve better performance.

4 Experiments and Results

4.1 Datasets

We used five datasets to comprehensively evaluate the performance of WENO, including two synthetic datasets and three real-world datasets. To explore the performance of WENO under different positive instance ratios, we used the 10-class natural image dataset CIFAR 10 [15] and the 9-class pathological image dataset CRC [14] to construct synthetic WSI datasets with different positive instance ratios, and they are denoted CIFAR-10-MIL dataset and the CRC-MIL dataset, respectively. Furthermore, we used real-world pathology datasets from three different medical centers to evaluate the performance of WENO, including a breast cancer lymph node metastasis public dataset, the Camelyon16 dataset [1], a lung cancer diagnosis public dataset, the TCGA Lung Cancer dataset, and an in-house cervical cancer lymph node metastasis dataset, the Clinical Cervical dataset. Detailed descriptions of the datasets are available in the supplementary material.

4.2 Evaluation Metrics

For both instance and bag classification, we use the Area Under Curve (AUC) as the evaluation metric. We report the AUC metrics for the instance and bag classification on two synthetic datasets and the Camelyon 16 dataset. However, since the instance-level ground truth labels for the TCGA Lung Cancer dataset and the Clinical Cervical dataset are not available, we only report their AUC for bag classification.

4.3 Implementation Details

For the CIFAR-10-MIL dataset, the encoder in Figure 2 is implemented using the AlexNet [16]. For the other datasets, the encoder is implemented using the ResNet18 [10]. Both the prediction heads and the attention module are implemented using fully connected layers. No pre-training of the network parameters and no image augmentation are performed. The SGD optimizer is used to optimize the network parameters with a fixed learning rate of 0.001. For the hard positive instance mining strategy, we drop the instances with positive probability higher than a threshold in positive bags. The hyperparameter thresholds vary for each dataset, and we used grid search on the validation set to determine the optimal values. In the supplementary material, we give a robustness study of the threshold on the Camelyon 16 dataset. All experiments were performed using 4 Nvidia 3090 GPUs.

4.4 Comparison Methods

We compare WENO with a series of state-of-the-art methods. For both the synthetic datasets and the real-world datasets, we use the classic ABMIL [13] and the latest DSMIL [18] as the teachers to construct the WENO frameworks and compare their instance and bag classification performance with SOTA methods. The comparison methods include instance-based methods: RNN-MIL [2] and

Chi-MIL [5]; bag-based methods: ABMIL [13], Loss-ABMIL [29] and DSMIL [18]. We reproduced these methods based on the published codes, and the specific parameter settings are provided in the supplementary material. We also compare the results of using the fully supervised approaches on the synthetic datasets and the Camelyon 16 dataset, i.e., performing supervised training using the true labels of each instance and aggregating the instance predictions using max-pooling to obtain the bag predictions.

4.5 Results on Synthetic Datasets

Table 1 and Table 2 show the instance and bag classification performance of WENO on the CIFAR-10-MIL dataset and the CRC-MIL dataset with different positive instance ratios, respectively. We use the classic ABMIL [13] and the latest DSMIL [18] as the teachers to construct the WENO frameworks. It can be seen that the WENO framework significantly improves the performance of the two original bag-based methods for both the bag classification and the instance classification tasks under all positive instance ratios. The advantage of WENO is especially significant for instance classification. In particular, DSMIL [18] does not work well in instance classification under low positive instance ratios, while the performance of DSMIL+WENO is much higher. For bag classification, as shown in Table 1 (b), DSMIL [18] does not work at positive instance ratios of 5% and 10%, while the bag classification AUC after combining the WENO framework reaches 0.9367 and 0.9900, respectively. These results show the powerful advantages of WENO: significant performance gains and easy plug-and-play ability.

Table 1: Results on the CIFAR-10-MIL dataset.

(a) Instance classification AUC.							(b) Bag classification AUC.						
Positive patch ratio	1%	5%	10%	20%	50%	70%	Positive patch ratio	1%	5%	10%	20%	50%	70%
Fully supervised	0.9215	0.9621	0.9723	0.9740	0.9699	0.9715	Fully supervised	0.5758	0.9531	0.9905	0.9972	1.000	1.000
ABMIL [13]	0.6253	0.9083	0.9241	0.9237	0.8224	0.7935	ABMIL [13]	0.5783	0.8850	0.9955	1.000	1.000	1.000
ABMIL + WENO	0.7427	0.9289	0.9492	0.9581	0.9495	0.9454	ABMIL + WENO	0.6005	0.9300	0.9973	1.000	1.000	1.000
Δ	+0.1174	+0.0206	+0.0251	+0.0344	+0.1271	+0.1519	Δ	+0.0222	+0.0450	+0.0018	-	-	-
DSMIL [18]	0.4039	0.5515	0.4918	0.8258	0.6152	0.7525	DSMIL [18]	0.4025	0.5174	0.5265	0.9468	0.9850	1.000
DSMIL + WENO	0.7291	0.9408	0.9179	0.9657	0.9393	0.9525	DSMIL + WENO	0.4069	0.9367	0.9900	1.000	1.000	1.000
Δ	+0.3252	+0.3893	+0.4261	+0.1399	+0.3241	+0.2000	Δ	+0.0044	+0.4193	+0.4635	+0.0532	+0.0150	-

Table 2: Results on the CRC-MIL dataset.

(a) Instance classification AUC.					(b) Bag classification AUC.				
Positive patch ratio	10%	20%	50%	70%	Positive patch ratio	10%	20%	50%	70%
Fully supervised	0.9978	0.9976	0.9977	0.9971	Fully supervised	1.000	1.000	1.000	1.000
ABMIL [13]	0.7410	0.8729	0.8800	0.7965	ABMIL [13]	0.9754	1.000	0.9766	0.9894
ABMIL + WENO	0.9625	0.9819	0.9759	0.9786	ABMIL + WENO	1.0000	1.000	0.9957	1.0000
Δ	+0.2215	+0.1090	+0.0959	+0.1821	Δ	+0.0246	-	+0.0191	+0.0106
DSMIL [18]	0.3690	0.7008	0.4835	0.7399	DSMIL [18]	1.000	0.8914	0.9997	1.000
DSMIL + WENO	0.9697	0.9801	0.9817	0.9760	DSMIL + WENO	1.000	1.0000	1.0000	1.000
Δ	+0.6007	+0.2793	+0.4982	+0.2361	Δ	-	+0.1086	+0.0003	-

4.6 Results on Real-World Datasets

Table 3 (a) shows the performance of WENO on the Camelyon16 dataset for the instance and bag classification. We still use ABMIL [13] and DSMIL [18] as the teachers to construct the WENO frameworks. It can be seen that using WENO brings a significant performance improvement in both classification tasks. Notably, with only bag-level weak labels, the best instance classification AUC (0.9377) obtained with WENO is lower than that of fully supervised method (0.9644) by only 0.0267; while the best bag classification AUC (0.8663) exceeds the fully supervised (0.8621) method, showing the powerful performance of WENO again.

Table 3 (b) shows the bag classification performance of WENO on the TCGA Lung Cancer dataset. We use ABMIL [13] and DSMIL [18] as the teachers to construct the WENO frameworks and achieve the best performance.

Table 3 (c) shows the bag classification performance of WENO on the Clinical Cervical dataset. We use ABMIL [13] and DSMIL [18] as the teachers to construct the WENO frameworks and achieve the optimal performance. In contrast to previous clinical tumor recognition and classification tasks,

the prediction of lymph node metastasis according to the WSIs of primary lesion in this dataset is a very challenging task in current clinical practice. Since there is no prior knowledge about what image features of the primary lesion indicate metastasis, even very experienced pathologists are unable to clearly distinguish between positive and negative instances. WENO achieves the best performance among all comparison methods, which on the one hand indicates that WENO can be applied to the prediction of metastasis using primary lesion WSIs in clinical practice, and on the other hand suggests the potential of WENO to detect underlying pathological patterns from high confident instances.

Some examples of positive and negative slides/patches in the three real-world datasets and the visualization of the heatmaps on the Camelyon16 dataset are given in the supplementary material.

Table 3: Results on the three real-world datasets.

(a) Camelyon16 Dataset.			(b) TCGA Lung Cancer Dataset.		(c) Clinical Cervical Dataset.	
Methods	Instance-level AUC	Bag-level AUC	Methods	Bag-level AUC	Methods	Bag-level AUC
Fully supervised	0.9644	0.8621	Mean-pooling	0.9369	Loss-ABMIL [29]	0.5833
Loss-ABMIL [29]	0.8995	0.7965	Max-pooling	0.9014	ChiMIL [5]	0.7425
ChiMIL [5]	0.7880	0.7025	RNN-MIL [2]	0.9107	ABMIL [13]	0.6446
ABMIL [13]	0.8480	0.8379	ABMIL [13]	0.9488	ABMIL + WENO	0.8056
ABMIL + WENO	0.9271	0.8663	ABMIL + WENO	0.9663	Δ	+0.1610
Δ	+0.0791	+0.0284	Δ	+0.0175	DSMIL [18]	0.8022
DSMIL [18]	0.8568	0.8401	DSMIL [18]	0.9633	DSMIL + WENO	0.8222
DSMIL + WENO	0.9377	0.8495	DSMIL + WENO	0.9727	Δ	+0.0200
Δ	+0.0809	+0.0094	Δ	+0.0094		

5 Ablation Study

Figure 3 shows the results of the ablation study of WENO on the CIFAR-10-MIL dataset with a positive instance ratio of 0.2. In this experiment, we use the ABMIL [13] as the teacher to construct the WENO framework. By analyzing the curves in Figure 3, we can find: (1) Comparing the curves of the raw 'ABMIL' and 'ABMIL+WENO (without HPM)' in panel (a) and panel (b), it can be seen that when the bag-level AUC reaches the maximum at about the 25th epoch, their instance-level classification ability is still poor. In addition, the instance-level AUC of the raw ABMIL gets worse as the training proceeds, indicating that the network gradually tends to distinguish positive bags by simple positive instances only. As shown in Figure 3 (b), when WENO is used with ABMIL, the instance-level classification capability is significantly improved, and the network is still able to continuously improve the instance classification capability as the training proceeds. 2) Comparing the curves of the 'ABMIL+WENO (without HPM)' and 'ABMIL+WENO (with HPM)' in panel (b) and panel (c), it can be seen that the proposed hard positive instance mining strategy can further improve the instance classification ability of both the student and the teacher by forcing the teacher network to continuously learn and mine hard positive instances in positive bags. HPM is used after the 150th epoch.

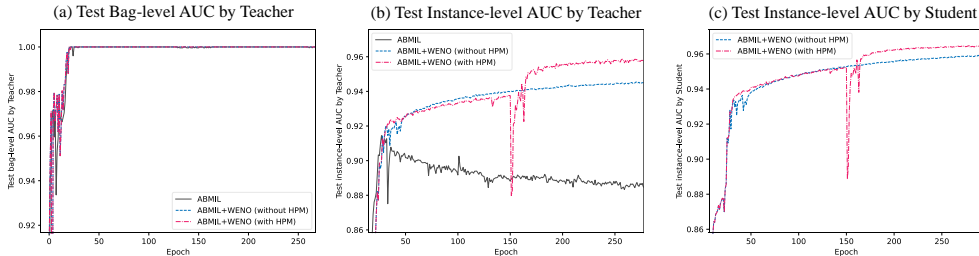


Figure 3: Ablation study curves on the CIFAR-10-MIL dataset.

Table 4 shows the results of the ablation study of key components of WENO on the Camelyon16 dataset. We construct the WENO framework with ABMIL [13] as the teacher, where 'Distillation' represents whether distillation is used (without 'Distillation' denotes the raw ABMIL), 'Shared Encoder' represents whether the encoders of the teacher and the student share parameters, and 'HPM' indicates whether hard instance mining strategy is performed or not. The AUCs of both instance and bag classification indicate the effectiveness of each component of WENO.

Table 4: Ablation study on the Camelyon16 Dataset.

Distillation	Shared Encoder	HPM	Instance-level AUC	Bag-level AUC
✓			0.8480	0.8379
✓	✓		0.8787	0.8574
✓	✓	✓	0.9271	0.8663

6 Visualization of the predictions on the Camelyon16 Dataset

Figure 4 shows some representative predictions on the Camelyon16 dataset. As can be seen, using only slide-level labels, our method is able to accurately predict almost all positive instances, regardless of whether there is a large or small proportion of positive regions in the WSIs. This intuitively demonstrates the powerful performance of WENO and its great potential for clinical applications.

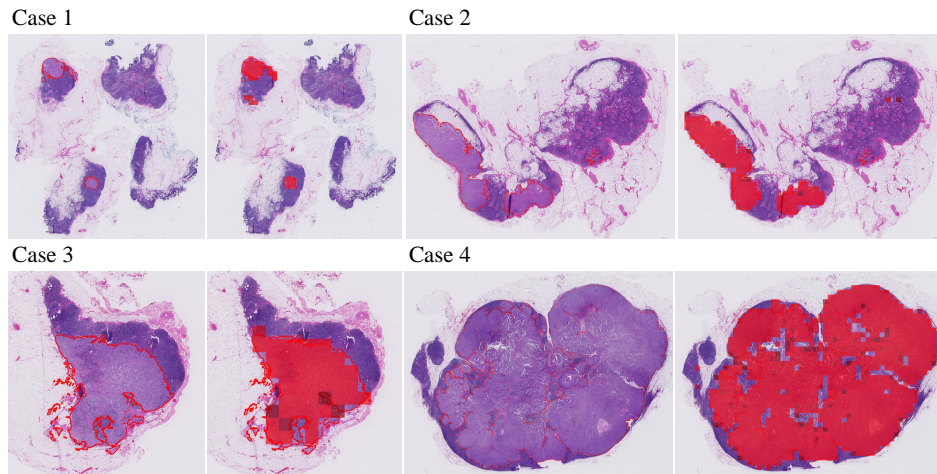


Figure 4: Visualization of the representative predictions on the Camelyon16 dataset, where four cases are included. For each case, the left image is the original image, where the contours of the ground truth positive regions are outlined using red lines and the right image is the predicted image, where the predicted positive instances are marked using red squares and the predicted negative instances are not marked.

7 Conclusion

In this paper, we propose WENO, an end-to-end weakly supervised knowledge distillation framework for whole slide image classification. WENO is a plug-and-play framework that can use any existing bag-based MIL methods using attention mechanism as the teacher branch and improves its performance on both bag and instance classification. WENO trains the student classifier with the normalized attention scores of the teacher branch through knowledge distillation, and uses the hard positive instance mining (HPM) strategy to force the teach network to further mine and learn from hard positive instances. In experiments, WENO shows strong instance and bag classification performance on all five datasets, reaching new SOTA. WENO also has the potential to be applied to other MIL problems. As for the limitations, the HPM strategy requires searching for optimal parameters on the validation set, which may prolong the training time. Deep learning-based WSI analysis has a long history, so our study has the same potential negative societal impacts as existing studies.

Acknowledgments

This work was supported by National Natural Science Foundation of China under Grant 82072021.

References

- [1] Babak Ehteshami Bejnordi, Mitko Veta, Paul Johannes Van Diest, Bram Van Ginneken, Nico Karssemeijer, Geert Litjens, Jeroen AWM Van Der Laak, Meyke Hermsen, Quirine F Manson, Maschenka Balkenhol, et al. Diagnostic assessment of deep learning algorithms for detection of lymph node metastases in women with breast cancer. *JAMA*, 318(22):2199–2210, 2017.
- [2] Gabriele Campanella, Matthew G Hanna, Luke Geneslaw, Allen Mirafior, Vitor Werneck Krauss Silva, Klaus J Busam, Edi Brogi, Victor E Reuter, David S Klimstra, and Thomas J Fuchs. Clinical-grade computational pathology using weakly supervised deep learning on whole slide images. *Nature Medicine*, 25(8):1301–1309, 2019.
- [3] Mathilde Caron, Hugo Touvron, Ishan Misra, Hervé Jégou, Julien Mairal, Piotr Bojanowski, and Armand Joulin. Emerging properties in self-supervised vision transformers. In *Proceedings of the IEEE/CVF International Conference on Computer Vision (ICCV)*, pages 9650–9660, 2021.
- [4] Veronika Cheplygina, Marleen de Bruijne, and Josien PW Pluim. Not-so-supervised: a survey of semi-supervised, multi-instance, and transfer learning in medical image analysis. *Medical Image Analysis*, 54:280–296, 2019.
- [5] Philip Chikontwe, Meejeong Kim, Soo Jeong Nam, Heounjeong Go, and Sang Hyun Park. Multiple instance learning with center embeddings for histopathology classification. In *International Conference on Medical Image Computing and Computer-Assisted Intervention (MICCAI)*, pages 519–528. Springer, 2020.
- [6] Inseop Chung, SeongUk Park, Jangho Kim, and Nojun Kwak. Feature-map-level online adversarial knowledge distillation. In *International Conference on Machine Learning (ICML)*, pages 2006–2015. PMLR, 2020.
- [7] Ji Feng and Zhi-Hua Zhou. Deep miml network. In *Proceedings of the AAAI Conference on Artificial Intelligence (AAAI)*, volume 31, 2017.
- [8] Jianping Gou, Baosheng Yu, Stephen J Maybank, and Dacheng Tao. Knowledge distillation: A survey. *International Journal of Computer Vision*, 129(6):1789–1819, 2021.
- [9] Noriaki Hashimoto, Daisuke Fukushima, Ryoichi Koga, Yusuke Takagi, Kaho Ko, Kei Kohno, Masato Nakaguro, Shigeo Nakamura, Hidekata Hontani, and Ichiro Takeuchi. Multi-scale domain-adversarial multiple-instance cnn for cancer subtype classification with unannotated histopathological images. In *Proceedings of the IEEE/CVF Conference on Computer Vision and Pattern Recognition (CVPR)*, pages 3852–3861, 2020.
- [10] Kaiming He, Xiangyu Zhang, Shaoqing Ren, and Jian Sun. Deep residual learning for image recognition. In *Proceedings of the IEEE Conference on Computer Vision and Pattern Recognition (CVPR)*, pages 770–778, 2016.
- [11] Byeongho Heo, Jeesoo Kim, Sangdoon Yun, Hyojin Park, Nojun Kwak, and Jin Young Choi. A comprehensive overhaul of feature distillation. In *Proceedings of the IEEE/CVF International Conference on Computer Vision (ICCV)*, pages 1921–1930, 2019.
- [12] Geoffrey Hinton, Oriol Vinyals, Jeff Dean, et al. Distilling the knowledge in a neural network. *arXiv preprint arXiv:1503.02531*, 2(7), 2015.
- [13] Maximilian Ilse, Jakob Tomczak, and Max Welling. Attention-based deep multiple instance learning. In *International Conference on Machine Learning (ICML)*, pages 2127–2136. PMLR, 2018.
- [14] Jakob Nikolas Kather, Cleo-Aron Weis, Francesco Bianconi, Susanne M Melchers, Lothar R Schad, Timo Gaiser, Alexander Marx, and Frank Gerrit Zöllner. Multi-class texture analysis in colorectal cancer histology. *Scientific Reports*, 6(1):1–11, 2016.
- [15] Alex Krizhevsky, Geoffrey Hinton, et al. Learning multiple layers of features from tiny images. 2009.

- [16] Alex Krizhevsky, Ilya Sutskever, and Geoffrey E Hinton. Imagenet classification with deep convolutional neural networks. *Advances in Neural Information Processing Systems (NeurIPS)*, 25, 2012.
- [17] Hankook Lee, Sung Ju Hwang, and Jinwoo Shin. Self-supervised label augmentation via input transformations. In *International Conference on Machine Learning (ICML)*, pages 5714–5724. PMLR, 2020.
- [18] Bin Li, Yin Li, and Kevin W Eliceiri. Dual-stream multiple instance learning network for whole slide image classification with self-supervised contrastive learning. In *Proceedings of the IEEE/CVF Conference on Computer Vision and Pattern Recognition (CVPR)*, pages 14318–14328, 2021.
- [19] Hang Li, Fan Yang, Yu Zhao, Xiaohan Xing, Jun Zhang, Mingxuan Gao, Junzhou Huang, Liansheng Wang, and Jianhua Yao. Dt-mil: Deformable transformer for multi-instance learning on histopathological image. In *International Conference on Medical Image Computing and Computer-Assisted Intervention (MICCAI)*, pages 206–216. Springer, 2021.
- [20] Xintong Li, Chen Li, Md Mamunur Rahaman, Hongzan Sun, Xiaoqi Li, Jian Wu, Yudong Yao, and Marcin Grzegorzec. A comprehensive review of computer-aided whole-slide image analysis: from datasets to feature extraction, segmentation, classification and detection approaches. *Artificial Intelligence Review*, pages 1–70, 2022.
- [21] Yufan Liu, Jiajiong Cao, Bing Li, Chunfeng Yuan, Weiming Hu, Yangxi Li, and Yunqiang Duan. Knowledge distillation via instance relationship graph. In *Proceedings of the IEEE/CVF Conference on Computer Vision and Pattern Recognition (CVPR)*, pages 7096–7104, 2019.
- [22] Ming Y Lu, Drew FK Williamson, Tiffany Y Chen, Richard J Chen, Matteo Barbieri, and Faisal Mahmood. Data-efficient and weakly supervised computational pathology on whole-slide images. *Nature Biomedical Engineering*, 5(6):555–570, 2021.
- [23] Andriy Myronenko, Ziyue Xu, Dong Yang, Holger R Roth, and Daguang Xu. Accounting for dependencies in deep learning based multiple instance learning for whole slide imaging. In *International Conference on Medical Image Computing and Computer-Assisted Intervention (MICCAI)*, pages 329–338. Springer, 2021.
- [24] Wonpyo Park, Dongju Kim, Yan Lu, and Minsu Cho. Relational knowledge distillation. In *Proceedings of the IEEE/CVF Conference on Computer Vision and Pattern Recognition (CVPR)*, pages 3967–3976, 2019.
- [25] Baoyun Peng, Xiao Jin, Jiaheng Liu, Dongsheng Li, Yichao Wu, Yu Liu, Shunfeng Zhou, and Zhaoning Zhang. Correlation congruence for knowledge distillation. In *Proceedings of the IEEE/CVF International Conference on Computer Vision (ICCV)*, pages 5007–5016, 2019.
- [26] Jérôme Rony, Soufiane Belharbi, Jose Dolz, Ismail Ben Ayed, Luke McCaffrey, and Eric Granger. Deep weakly-supervised learning methods for classification and localization in histology images: a survey. *arXiv preprint arXiv:1909.03354*, 2019.
- [27] Zhuchen Shao, Hao Bian, Yang Chen, Yifeng Wang, Jian Zhang, Xiangyang Ji, et al. Transmil: Transformer based correlated multiple instance learning for whole slide image classification. *Advances in Neural Information Processing Systems (NeurIPS)*, 34, 2021.
- [28] Yash Sharma, Aman Shrivastava, Lubaina Ehsan, Christopher A Moskaluk, Sana Syed, and Donald Brown. Cluster-to-conquer: A framework for end-to-end multi-instance learning for whole slide image classification. In *Medical Imaging with Deep Learning*, pages 682–698. PMLR, 2021.
- [29] Xiaoshuang Shi, Fuyong Xing, Yuanpu Xie, Zizhao Zhang, Lei Cui, and Lin Yang. Loss-based attention for deep multiple instance learning. In *Proceedings of the AAAI Conference on Artificial Intelligence (AAAI)*, volume 34, pages 5742–5749, 2020.
- [30] Chetan L Srinidhi, Ozan Ciga, and Anne L Martel. Deep neural network models for computational histopathology: A survey. *Medical Image Analysis*, 67:101813, 2021.

- [31] Xi Wang, Hao Chen, Caixia Gan, Huangjing Lin, Qi Dou, Efstratios Tsougenis, Qitao Huang, Muyan Cai, and Pheng-Ann Heng. Weakly supervised deep learning for whole slide lung cancer image analysis. *IEEE Transactions on Cybernetics*, 50(9):3950–3962, 2019.
- [32] Xinggang Wang, Yongluan Yan, Peng Tang, Xiang Bai, and Wenyu Liu. Revisiting multiple instance neural networks. *Pattern Recognition*, 74:15–24, 2018.
- [33] Jiajun Wu, Yinan Yu, Chang Huang, and Kai Yu. Deep multiple instance learning for image classification and auto-annotation. In *Proceedings of the IEEE Conference on Computer Vision and Pattern Recognition (CVPR)*, pages 3460–3469, 2015.
- [34] Ting-Bing Xu and Cheng-Lin Liu. Data-distortion guided self-distillation for deep neural networks. In *Proceedings of the AAAI Conference on Artificial Intelligence (AAAI)*, volume 33, pages 5565–5572, 2019.
- [35] Yan Xu, Jun-Yan Zhu, Eric Chang, and Zhuowen Tu. Multiple clustered instance learning for histopathology cancer image classification, segmentation and clustering. In *2012 IEEE Conference on Computer Vision and Pattern Recognition (CVPR)*, pages 964–971. IEEE, 2012.
- [36] Jiawen Yao, Xinliang Zhu, Jitendra Jonnagaddala, Nicholas Hawkins, and Junzhou Huang. Whole slide images based cancer survival prediction using attention guided deep multiple instance learning networks. *Medical Image Analysis*, 65:101789, 2020.
- [37] Sukmin Yun, Jongjin Park, Kimin Lee, and Jinwoo Shin. Regularizing class-wise predictions via self-knowledge distillation. In *Proceedings of the IEEE/CVF Conference on Computer Vision and Pattern Recognition (CVPR)*, pages 13876–13885, 2020.
- [38] Xinliang Zhu, Jiawen Yao, Feiyun Zhu, and Junzhou Huang. Wsisa: Making survival prediction from whole slide histopathological images. In *Proceedings of the IEEE Conference on Computer Vision and Pattern Recognition (CVPR)*, pages 7234–7242, 2017.

Checklist

1. For all authors...
 - (a) Do the main claims made in the abstract and introduction accurately reflect the paper’s contributions and scope? [\[Yes\]](#)
 - (b) Did you describe the limitations of your work? [\[Yes\]](#) See Section 7.
 - (c) Did you discuss any potential negative societal impacts of your work? [\[Yes\]](#) See Section 7.
 - (d) Have you read the ethics review guidelines and ensured that your paper conforms to them? [\[Yes\]](#)
2. If you are including theoretical results...
 - (a) Did you state the full set of assumptions of all theoretical results? [\[N/A\]](#)
 - (b) Did you include complete proofs of all theoretical results? [\[N/A\]](#)
3. If you ran experiments...
 - (a) Did you include the code, data, and instructions needed to reproduce the main experimental results (either in the supplemental material or as a URL)? [\[No\]](#) Code will be publicly available.
 - (b) Did you specify all the training details (e.g., data splits, hyperparameters, how they were chosen)? [\[Yes\]](#) See Section 4.3.
 - (c) Did you report error bars (e.g., with respect to the random seed after running experiments multiple times)? [\[No\]](#)
 - (d) Did you include the total amount of compute and the type of resources used (e.g., type of GPUs, internal cluster, or cloud provider)? [\[Yes\]](#) See Section 4.3.
4. If you are using existing assets (e.g., code, data, models) or curating/releasing new assets...
 - (a) If your work uses existing assets, did you cite the creators? [\[Yes\]](#) See Section 4.1.
 - (b) Did you mention the license of the assets? [\[No\]](#)

- (c) Did you include any new assets either in the supplemental material or as a URL? [No]
 - (d) Did you discuss whether and how consent was obtained from people whose data you're using/curating? [No]
 - (e) Did you discuss whether the data you are using/curating contains personally identifiable information or offensive content? [No]
5. If you used crowdsourcing or conducted research with human subjects...
- (a) Did you include the full text of instructions given to participants and screenshots, if applicable? [N/A]
 - (b) Did you describe any potential participant risks, with links to Institutional Review Board (IRB) approvals, if applicable? [N/A]
 - (c) Did you include the estimated hourly wage paid to participants and the total amount spent on participant compensation? [N/A]

Supplementary Material

Linhao Qu*

Digital Medical Research Center,
School of Basic Medical Science,
Fudan University
lhqu20@fudan.edu.cn

Xiaoyuan Luo*

Digital Medical Research Center,
School of Basic Medical Science,
Fudan University
19111010030@fudan.edu.cn

Manning Wang†

Digital Medical Research Center,
School of Basic Medical Science,
Fudan University
mnwang@fudan.edu.cn

Zhijian Song†

Digital Medical Research Center,
School of Basic Medical Science,
Fudan University
zjsong@fudan.edu.cn

The supplementary material consists of four sections. Section 1 introduces the details of the five datasets, section 2 shows the robustness study of the threshold of the hard positive instance mining (HPM) strategy on the Camelyon16 dataset, section 3 shows the robustness study of the starting epoch of HPM strategy on the CIFAR-10-MIL dataset and section 4 focuses on the specific parameter settings of the comparison methods.

1 Details of the Five Datasets

1.1 Synthetic Datasets

To evaluate the performance of WENO under different positive instance ratios and compare it with SOTA algorithms, we used the 10-class natural image dataset CIFAR-10 [6] and the 9-class pathological image dataset CRC-100K [5] to construct WSI datasets with different positive instance ratios, namely CIFAR-10-MIL dataset and CRC-MIL dataset, respectively.

CIFAR-10-MIL Dataset. The CIFAR-10 dataset [6] consists of 60000 32×32 color images in 10 classes (airplane, automobile, bird, cat, deer, dog, frog, horse, ship, truck), with 6000 images per class. There are 50000 training images and 10000 testing images. To simulate the pathological Whole Slide Image (WSI), we combined a random set of images from each of the 10 categories in the CIFAR-10 dataset to construct a WSI. Specifically, we considered each image of each category in the CIFAR-10 dataset as an instance, where only all instances of the "truck" category were labeled as positive and other instances as negative (the truck category was randomly selected). Then, we randomly selected a positive instances and $100 - a$ negative instances from all instances without replacement to form a positive bag with a positive instance ratio of $\frac{a}{100}$. Similarly, we randomly selected 100 negative instances without replacement to form a negative bag. This process was repeated until all the positive or negative instances in the CIFAR-10 dataset were used up. By adjusting the value of a , we constructed six subsets of the CIFAR-10-MIL dataset, and the positive instance ratios of the six subsets were 1%, 5%, 10%, 20%, 50%, and 70%, respectively. The number of bags in the training and testing sets on the CIFAR-10-MIL dataset under different positive instance ratios is shown in Table 1. Figure 1 shows the representative synthetic WSIs of the CIFAR-10-MIL dataset under each positive instance ratio.

CRC-MIL Dataset. The CRC-100K dataset [5] is a real pathology image dataset containing 100,000 images of human colorectal cancer and healthy tissue with detailed category annotation. The dataset is

*Equal Contribution.

†Corresponding Authors

Table 1: The number of bags in the training and testing sets on the CIFAR-10-MIL dataset under different positive instance ratios.

Positive instance ratio	1%	5%	10%	20%	50%	70%
Num of bags (train: test)	452:90	459:91	472:94	500:100	200:40	142:28

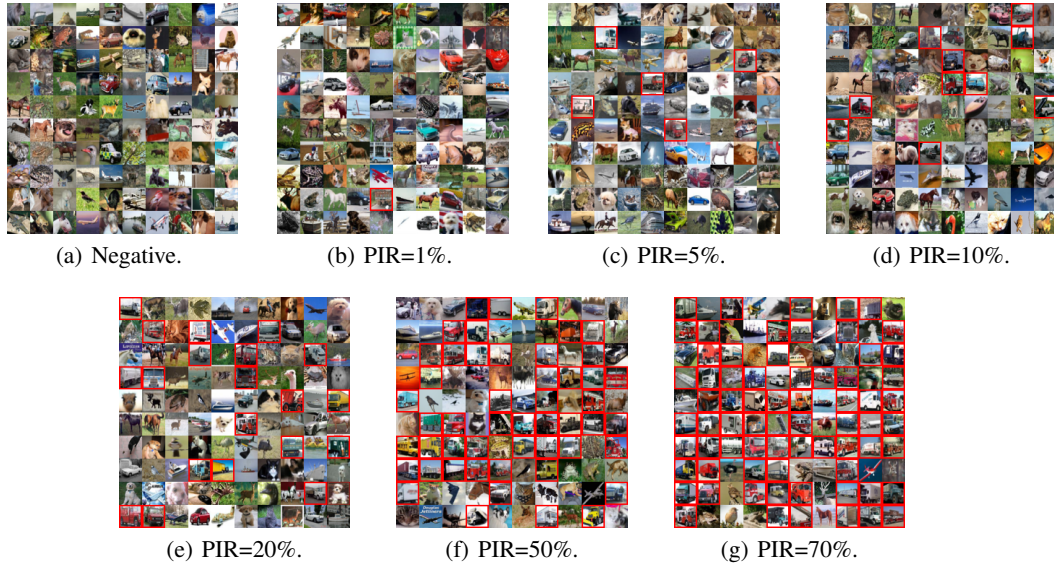


Figure 1: Examples of representative synthetic WSIs of CIFAR-10-MIL dataset, including a negative slide and six positive slides with positive instance ratio (PIR) of 1%, 5%, 10%, 20%, 50% and 70%. The positive instances in each slide are marked by red boxes.

sampled at $20\times$ magnification for 224×224 patches and contains the following nine non-overlapping pathology categories, namely adipose, background, debris, lymphocytes, mucus, smooth muscle, normal colon mucosa, cancer-associated stroma, and colorectal adenocarcinoma epithelium. We used the CRC-100K dataset to construct the CRC-MIL dataset with different positive instance ratios. Consistent with the CIFAR-10-MIL dataset, we set all instances in the category "colorectal adenocarcinoma epithelium" as positive instances and the remaining instances as negative instances. We randomly selected a positive instances and $100 - a$ negative instances from all instances without replacement to form a positive bag with a positive instance ratio of $\frac{a}{100}$. Similarly, we randomly selected 100 negative instances without replacement to form a negative bag. This process was repeated until all the positive or negative instances in the CRC-100K dataset were used up. By adjusting the value of a , we constructed four subsets of the CRC-MIL dataset and the positive instance ratios of the four subsets were 10%, 20%, 50% and 70%, respectively. The number of bags in the training and testing sets on the CRC-MIL dataset under different positive instance ratios is shown in Table 2. Figure 2 shows some examples of representative synthetic WSIs of the CRC-MIL dataset.

Table 2: The number of bags in the training and testing sets on the CRC-MIL dataset under different positive instance ratios.

Positive instance ratio	10%	20%	50%	70%
Num of bags (train: test)	720:180	760:190	458:114	326:80

1.2 Real-World Datasets

We used three real-world datasets from three different centers to evaluate the performance of WENO in real-world pathology diagnosis. The real-world datasets contain a breast cancer lymph node metastasis public dataset, Camelyon16 dataset [1], a lung cancer diagnosis public dataset, TCGA

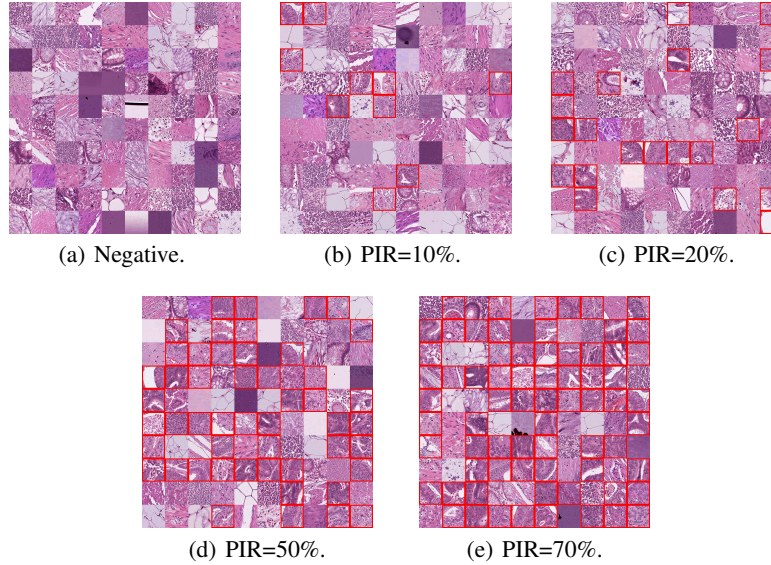


Figure 2: Examples of representative synthetic WSIs of CRC-MIL dataset, including a negative slide and four positive slides with positive instance ratio (PIR) of 10%, 20%, 50% and 70%. The positive instances in each slide are marked by red boxes.

Lung Cancer dataset, and a cervical cancer lymph node metastasis in-house dataset, Clinical Cervical dataset.

Camelyon16 Dataset. Camelyon16 dataset is a public histopathology image dataset for detecting breast cancer metastasis in lymph nodes [1], and the dataset contains 400 WSIs of lymph nodes (270 for training and 130 for testing). The WSIs that contained metastasis were labeled positive, and the others were labeled negative. The dataset provides not only the labels of whether a WSI is positive but also pixel-level labels of the metastasis areas. We only used the slide-level labels for training to satisfy the weakly supervised scenarios, and used the pixel-level labels of cancer areas to evaluate the instance classification performance of each algorithm. For preprocessing, we divide each WSI into 512×512 image patches without overlapping under $5 \times$ magnification. Similar to DSMIL [7], patches with an entropy less than 5 are dropped out as background. A patch is labeled as positive if it contains 25% or more cancer areas; otherwise, it is labeled as negative. Finally, a total of 186,604 instances were obtained, of which there were only 8117 positive instances (4.3%). The number of positive instances in different positive bags varied greatly, and some positive bags contained only several positive instances. Figure 3 provides some representative examples of WSIs in the Camelyon16 dataset.

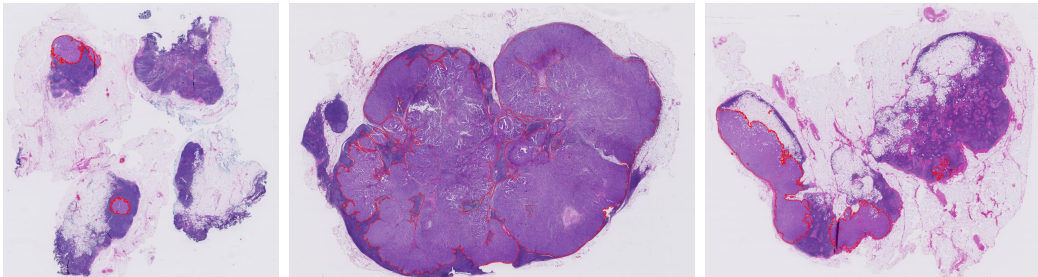


Figure 3: Visualization of some representative examples of WSIs in the Camelyon16 dataset. The images are original positive WSIs with different sizes of positive areas, which are outlined by red lines.

TCGA Lung Cancer Dataset. The TCGA Lung Cancer dataset includes a total of 1054 WSIs from The Cancer Genome Atlas (TCGA) Data Portal, which includes two sub-types of lung cancer, namely

Lung Adenocarcinoma and Lung Squamous Cell Carcinoma. Our goal is to accurately classify the two subtypes, where WSIs of Lung Adenocarcinoma are labeled as negative and WSIs of Lung Squamous Cell Carcinoma are labeled as positive. Only slide-level labels are available for this dataset, and patch-level labels are unknown. This dataset contains about 5.2 million patches at $20\times$ magnification, with an average of about 5,000 patches per bag. DSMIL [7] further mapped these patches to 512-dimensional features using contrastive self-supervised learning SimCLR [2]. Our experimental settings were exactly the same as DSMIL [7] and the features provided by DSMIL were used as input. We randomly divided the features of these WSIs into a training set (a total of 840 features) and a test set (a total of 210 features). Figure 4 shows some representative examples of WSIs in the TCGA Lung Cancer dataset.

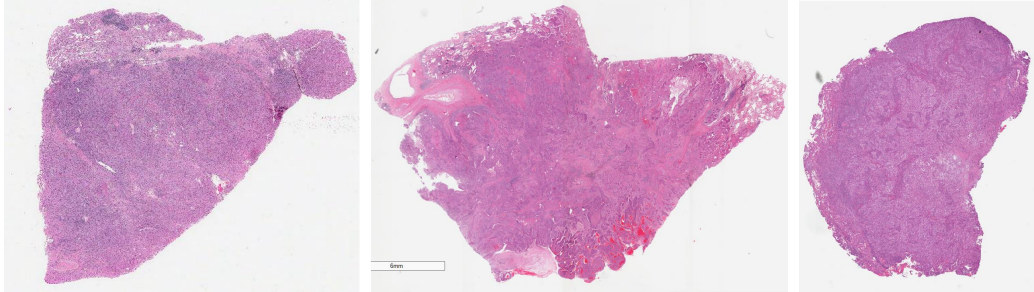


Figure 4: Visualization of some representative examples of WSIs in the TCGA Lung Cancer dataset.

Clinical Cervical Dataset. Clinical Cervical Dataset is an inhouse cervical cancer primary lesion pathology dataset that is used to directly predict a patient’s pelvic (including para-aortic) lymph node metastasis status from their primary lesion pathology slides. This is a pressing clinical challenge because of its clinical importance for the choice of treatment modality for patients. Unlike the two previous real-world datasets, this task is particularly difficult because there is no prior knowledge about what image features of the primary lesion indicate metastasis, even very experienced pathologists are unable to clearly distinguish between positive and negative instances. This dataset includes a total of 374 WSIs from different patients with cervical cancer, among which those with pelvic lymph node metastasis are labeled as positive (209 cases) and those without pelvic lymph node metastasis are labeled as negative (165 cases). We randomly divided the WSIs into a training set (300 cases) and a test set (74 cases) with an approximate ratio of 4:1, and the WSI was pre-processed in a similar way to Camelyon16, including removing the background regions and dividing the slides into 224×224 patches at $5\times$ magnification. Finally, 297,831 patches are obtained after preprocessing. Figure 5 provides some representative examples of WSIs in the Clinical Cervical Dataset.

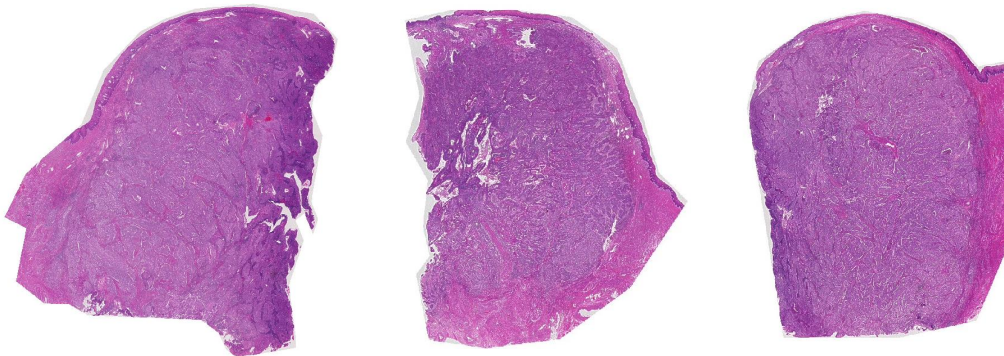


Figure 5: Visualization of some representative examples of WSIs in the Clinical Cervical dataset.

2 Robustness Study of the Threshold of the Hard Positive Instance Mining Strategy on the Camelyon16 Dataset

We propose the hard positive instance mining (HPM) strategy to force the teacher network to continuously learn and mine hard positive instances in the positive bags. Specifically, we first train the teacher and the student models for a certain number of epochs, after which the student network has a certain instance classification capability. Then, before continuing to train the teacher, we use the student classifier to predict all the instances in the input positive bags, and drop the instances with positive probability higher than a threshold in positive bags to construct hard pseudo bags. We study the robustness of WENO to this threshold on the Camelyon16 dataset, and the results are shown in Table 3. We used the ABMIL [4] to construct the WENO framework. In the table, "w/o HPM" means that HPM strategy is not used and "w/ HPM" means that HPM strategy is used. When threshold=1.00, it is equivalent to not using the HPM strategy. It can be seen that the instance-level AUC with HPM strategy is significantly higher than that without HPM strategy at all thresholds; when the threshold is below 0.92, the bag-level AUC with HPM strategy is slightly lower than without HPM strategy, which may be caused by dropping too many positive instances. The instance-level AUC and bag-level AUC using HPM strategy are higher than the raw ABMIL at all thresholds. It can be seen that the optimal threshold is actually a trade-off between instance-level AUC and bag-level AUC, and we finally selected threshold=0.94 as the optimal threshold. The above robustness study also shows that the HPM strategy has a strong robustness.

Table 3: Robustness study of the threshold on the Camelyon16 dataset.

Method	Threshold	Instance-level AUC	Bag-level AUC
ABMIL [4]	-	0.8480	0.8379
ABMIL+WENO (w/o HPM)	1.0000	0.8787	0.8574
ABMIL+WENO (w/ HPM)	0.9800	0.8884	0.8717
ABMIL+WENO (w/ HPM)	0.9600	0.9196	0.8675
ABMIL+WENO (w/ HPM)	0.9400	0.9271	0.8663
ABMIL+WENO (w/ HPM)	0.9200	0.9256	0.8402
ABMIL+WENO (w/ HPM)	0.9000	0.9204	0.8495
ABMIL+WENO (w/ HPM)	0.8800	0.9042	0.8478

3 Robustness Study of the Starting Epoch of HPM Strategy on the CIFAR-10-MIL Dataset

We performed a robustness study on the starting epoch of the HPM strategy, and the results are shown in Figure 6. We construct the WENO framework using ABMIL [4] as the teacher and experimented on the CIFAR-10-MIL dataset with a positive instance ratio of 0.2. In the Figure, panel (a) represents the AUC metric for bag-level classification using the teacher network, panel (b) represents the AUC metric for instance-level classification using the normalized attention scores of the teacher network, and panel (c) represents the AUC metric for instance-level classification using the student network. The gray line (WENO + 100 epoch HPM) indicates that the HPM module is introduced at the 100th epoch, the blue line (WENO + 150 epoch HPM) indicates that the HPM module is introduced at the 150th epoch, and the red line (WENO + 200 epoch HPM) indicates that the HPM module is introduced at the 200th epoch. Comparing the gray, blue and red lines in panel (a), panel (b) and panel (c), it can be seen that there is little difference in the final performance regarding the bag-level classification and instance-level classification, whether HPM is introduced at the 100th, 150th and 200th epochs. In this experiment, we added HPM strategy at three different time point, the 100th, 150th and 200th epoch, and the results show that their final instance-level classification AUC of are almost the same for both the teacher and the student network. These results indicate that HPM is not sensitive to the starting epoch.

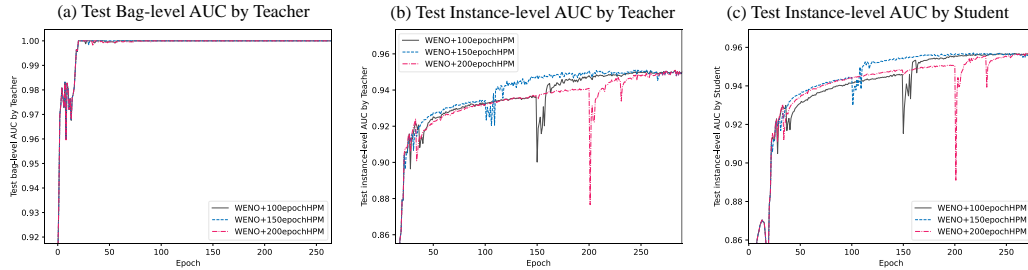


Figure 6: Robustness Study of the Starting Epoch of the HPM Strategy on the CIFAR-10-MIL dataset.

4 Specific Parameter Settings of the Comparison Methods

For all datasets except the TCGA Lung Cancer dataset, we performed a grid search on the key hyperparameters in all the comparison methods. For all comparison methods, we search learning rate over $\{0.0001, 0.0005, 0.001, 0.005, 0.01\}$. For Chi-MIL [3], we also search hyperparameter k over grid $\{2, 4, 8, 16, 32, 64\}$. For Loss-ABMIL [8], we search hyperparameter λ over grid $\{0.01, 0.1, 1, 10\}$. For the TCGA Lung Cancer dataset, since our experimental settings and inputs are exactly the same as those of DSMIL [7], we directly report the experimental results and comparison methods of DSMIL [7].

References

- [1] Babak Ehteshami Bejnordi, Mitko Veta, Paul Johannes Van Diest, Bram Van Ginneken, Nico Karssemeijer, Geert Litjens, Jeroen AWM Van Der Laak, Meyke Hermesen, Quirine F Manson, Maschenka Balkenhol, et al. Diagnostic assessment of deep learning algorithms for detection of lymph node metastases in women with breast cancer. *Jama*, 318(22):2199–2210, 2017.
- [2] Ting Chen, Simon Kornblith, Mohammad Norouzi, and Geoffrey Hinton. A simple framework for contrastive learning of visual representations. In *International Conference on Machine Learning (ICML)*, pages 1597–1607. PMLR, 2020.
- [3] Philip Chikontwe, Meejeong Kim, Soo Jeong Nam, Heounjeong Go, and Sang Hyun Park. Multiple instance learning with center embeddings for histopathology classification. In *International Conference on Medical Image Computing and Computer-Assisted Intervention (MICCAI)*, pages 519–528. Springer, 2020.
- [4] Maximilian Ilse, Jakub Tomczak, and Max Welling. Attention-based deep multiple instance learning. In *International Conference on Machine Learning (ICML)*, pages 2127–2136. PMLR, 2018.
- [5] Jakob Nikolas Kather, Cleo-Aron Weis, Francesco Bianconi, Susanne M Melchers, Lothar R Schad, Timo Gaiser, Alexander Marx, and Frank Gerrit Zöllner. Multi-class texture analysis in colorectal cancer histology. *Scientific Reports*, 6(1):1–11, 2016.
- [6] Alex Krizhevsky, Geoffrey Hinton, et al. Learning multiple layers of features from tiny images. 2009.
- [7] Bin Li, Yin Li, and Kevin W Eliceiri. Dual-stream multiple instance learning network for whole slide image classification with self-supervised contrastive learning. In *Proceedings of the IEEE/CVF Conference on Computer Vision and Pattern Recognition (CVPR)*, pages 14318–14328, 2021.
- [8] Xiaoshuang Shi, Fuyong Xing, Yuanpu Xie, Zizhao Zhang, Lei Cui, and Lin Yang. Loss-based attention for deep multiple instance learning. In *Proceedings of the AAAI Conference on Artificial Intelligence (AAAI)*, volume 34, pages 5742–5749, 2020.